Available online at www.sciencedirect.com
SCIENCE DIRECT®
Journal of Power Sources 132 (2004) 172–180
JOURNAL OF POWER SOURCES
www.elsevier.com/locate/jpowsour

A simple mechano-thermal coating process for improved lithium battery cathode materials

George Ting-Kuo Fey [a,*], Hao-Zhong Yang [a], T. Prem Kumar [a,1], Sajo P. Naik [a], Anthony S.T. Chiang [a], Dzu-Chi Lee [b], Jinn-Ren Lin [b]

[a] *Department of Chemical and Materials Engineering, National Central University, Chung-Li 32054, Taiwan, ROC*
[b] *Industrial Technology Research Institute 195, Section 4, Chung Hsing Road, Chu Tung, Hsin-chu 310, Taiwan, ROC*

Received 22 September 2003; received in revised form 7 January 2004; accepted 16 January 2004

Abstract

A simple, economical and convenient mechano-thermal coating procedure for the production of $LiCoO_2$ with improved cycling performance is described. The coating material was pre-formed nanoparticulate fumed silica. TEM studies with a 1.0 wt.% silica-coated cathode suggested that the silica species partially diffused into the bulk of the cathode material. XRD studies showed a diminished lattice parameter *c* upon coating, indicating that a substitutional compound of the $LiSi_yCo_{1-y}O_{2+0.5y}$ type might have formed upon calcination. SEM images, *R*-factor values from XRD studies and electrochemical studies showed that a coating level of 1.0 wt.% gave an optimal performance in capacity and cyclability. SEM images showed that above this level, the excess silica formed spherules, which got glued to the coated cathode particles. Galvanostatic cycling studies showed that at a coating level of 1.0 wt.%, cyclability improved three and nine times for two commercial $LiCoO_2$ samples.

Keywords: Coated cathodes; Mechano-thermal coating; Coated $LiCoO_2$; Fumed silica; Lithium-ion battery

1. Introduction

Lithiated transition metal oxides of the general formula $LiMO_2$, where M is a transition metal like V, Cr, Fe, Co or Ni, adapt the hexagonal α-$NaFeO_2$-type structure, in which the transition metal ions reside in the octahedral interstitial sites in a cubic closely-packed array of oxygen atoms in such a way that the MO_2 layers are formed by edge-sharing $[MO_6]$ octahedra. The lithium ions are present in octahedral $[LiO_6]$ coordination between these MO_2 layers. The high electronegativity of oxygen results in repulsive interactions between adjacent layers, which are compensated by the cations residing between the layers [1,2]. Thus, complete delithiation of these oxides results in thermodynamically unstable MO_2 compositions, which assume the layered $CdCl_2$-type structure. Among these *iso*-structural oxides, only $LiCoO_2$, $LiNiO_2$ and their solid solutions, $LiNi_{1-y}Co_yO_2$, have attained industrial importance as cathode-active materials in lithium batteries. $LiCoO_2$ is by far the most exploited because of its features like high voltages versus lithium, a theoretical specific capacity of 274 mAh/g, and good cycling features. Furthermore, it can be easily prepared by a variety of synthetic approaches.

The deintercalation of lithium from $LiCoO_2$ is accompanied by an expansion of the hexagonal lattice in the *c*-direction, as a result of the increased electrostatic repulsion between adjacent oxygen layers [3,4], and a contraction in the Co–Co distance [5,6]. This anisotropic volume change during repeated cycling causes a structural degradation of the host material [7] which results in large capacity fades [8,9]. Based on their ab initio calculations, Ceder et al. [10] suggested that doping $LiCoO_2$ with non-transition metal ions could improve the structural characteristics of the compound. Accordingly, several studies have been made on the effect of doping of $LiCoO_2$ with such dopants as Al^{3+} [11–13], Mg^{2+} [14,15] and B^{3+} [16]. However, in some cases, the structural stability degraded upon cycling, while in others, any improvement in structural stability was obtained at the expense of the deliverable capacity. In recent years, an alternative approach has been adopted to enhance the cyclability of cathode materials, wherein the cathode particles are coated with a thin film of oxide materials such

* Corresponding author. Tel.: +886-3-425-7325/422-7151x4206; fax: +886-3-425-7325.
E-mail address: gfey@cc.ncu.edu.tw (G.T.-K. Fey).
[1] On deputation from: Central Electrochemical Research Institute, Karaikudi 630006, TN, India.

0378-7753/$ – see front matter © 2004 Elsevier B.V. All rights reserved.
doi:10.1016/j.jpowsour.2004.01.033

as Al_2O_3 [17–19], B_2O_3 [19], MgO [20,21], SnO_2 [22], TiO_2 [19] and ZrO_2 [19]. Some authors suggest that the coating materials form substitutional oxides on the cathode surface, which bestow improved structural stability to the core material, enhancing its cyclability [21]. Cho et al. [19] suggest that coatings with high fracture-tough materials suppress the cycle-limiting phase transitions associated with the intercalation–deintercalation processes.

The coating procedures adopted in the above studies were based on the sol–gel technique, in which the oxide formed by the hydrolysis of a metal alkoxide was deposited in situ, followed by a calcination step. Although surface coating can also be accomplished by a variety of other techniques such as mechanical milling, dip-coating, spin coating, layer-by-layer coating, electrochemical deposition, chemical or electroless deposition, chemical and physical vapor deposition, spray pyrolysis, pulsed laser deposition, magnetron sputtering, self-assembly, plasma-assisted coating, etc., not all of them can be applied for particulate substrates. Most of these techniques require specialized equipment, which makes the coating process expensive. In a departure from conventional processes, we have adopted a simple, economical and convenient process by which pre-formed nanoparticles of the coating material are deposited on cathode powders in an attempt to obtain high-cycling coated cathodes. In this paper, we describe a simple mechano-thermal coating process for the production of coated cathode particles, and the physico-chemical and electrochemical cycling performance of the coated materials. The fumed silica coating material and the $LiCoO_2$ cathode samples were from commercial sources.

2. Experimental

A weighed amount of fumed silica (grade Cab-*o*-Sil P-1000 from Cabot Co.) of particle size 18 nm, was dispersed in ethanol by a 1 h sonication followed by 10 h of vigorous stirring. A commercial sample of $LiCoO_2$ (Com-A supplied by Coremax Taiwan Corporation) was added to this dispersion such that the weight ratios of the fumed silica to the cathode material were 0.3:99.7, 1.0:99.0, 3.0:97.0 and 5.0:95.0. The mixture was sonicated for 30 min, and stirred on a magnetic stirrer for 24 h. A subsequent slow evaporation of the solvent at 50 °C resulted in a black dry mass of fumed silica-coated $LiCoO_2$ particles. The coated particles were calcined at 450 °C for 10 h in order to ensure complete adhesion of the coated particles with the core material. The coating procedure is schematically represented in Fig. 1.

An X-ray diffractometer (Siemens D-5000, Mac Science MXP18) equipped with a nickel-filtered Cu Kα radiation source was used for structural analysis. The diffraction patterns were recorded between scattering angles of 5 and 80° in steps of 0.05°. BET surface area and particle size measurements were carried out on a Micromeritics ASAP 2010 surface area analyzer at 77 K. Prior to the measurements,

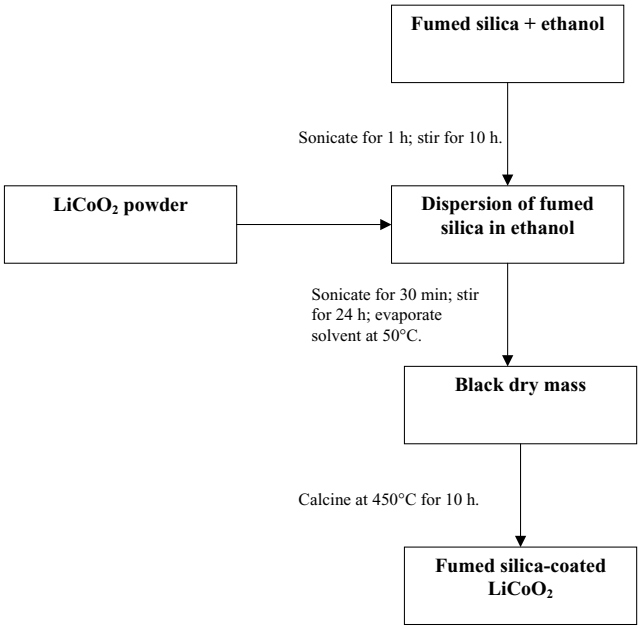

Fig. 1. Schematic of the mechano-thermal coating process.

the fumed silica sample was degassed for 12 h at 250 °C under 10^{-6} Torr. The surface area of the coating material was 165 $m^2\,g^{-1}$ and its average particle size was calculated to be 18 nm. The surface morphology of the coated materials was examined by scanning electron microscopy (Hitachi model S-3500V). The microstructures of the coated particles were examined by a JEOL JEM-200FXII transmission electron microscope equipped with a LaB_6 gun. The samples for TEM studies were prepared by dispersing the coated powders in ethanol, placing a drop of the clear solution on a carbon-coated copper grid, and subsequent drying. Depth profiles of silicon, cobalt and oxygen in the coated materials were recorded by ESCA (VG Scientific ESCALAB 250) in order to analyze the spatial distribution of the ions in the cathode particles.

Coin cells of the 2032 configuration were assembled in an argon-filled VAC MO40-1 glove box in which the oxygen and water contents were maintained below 2 ppm. Lithium metal (Foote Mineral) was used as the anode and a 1 M solution of $LiPF_6$ in EC:DEC (1:1 (v/v)) (Tomiyama Chemicals) was used as the electrolyte. The cathode was prepared by blade-coating a slurry of 85 wt.% coated active material with 10 wt.% conductive carbon black and 5 wt.% poly(vinylidene fluoride) binder in *N*-methyl-2-pyrrolidone on an aluminum foil, drying overnight at 120 °C in an oven, roller-pressing the dried coated foil, and punching out circular discs. The cells were cycled at 0.1 or 0.2*C* rate (with respect to a theoretical capacity of 274 mAh/g) between 2.75 and 4.40 V in a multi-channel battery tester (Maccor 4000). Phase transitions occurring during the cycling processes were examined by a slow scan cyclic voltammetric experiment, performed with a three-electrode glass cell. The working electrodes were prepared with the cathode pow-

ders as described above, but coated on both sides of the aluminum foil. The cells for the cyclic voltammetric studies were assembled inside the glove box with lithium metal foil serving as both counter and reference electrodes. The electrolyte used was the same as that for the coin cell. Cyclic voltammograms were run on a Solartron 1287 Electrochemical Interface at a scan rate of 0.1 mV/s between 3.0 and 4.4 V.

3. Results and discussion

3.1. X-ray diffraction

The X-ray diffraction patterns of the bare and coated Com-A $LiCoO_2$ powders (Fig. 2) conform to the $R\bar{3}m$ symmetry of the core material. The fact that no diffraction patterns corresponding to the silica coating material are observed is expected since fumed silica is amorphous. Table 1 shows that the lattice constants a and c of the coated materials are less than those for the uncoated sample, suggesting that the phases on the surface of the powder are solid solutions formed by the reaction of the silica particles with the core material. It is possible that during the 10 h calcination process a substitutional compound like $LiSi_yCo_{1-y}O_{2+0.5y}$ could have formed through the interaction of the silica with the substrate. The contraction in the c parameter may indicate such a possibility. Similar inter-oxide surface compositions have been proposed by other researchers too [17,21,23,24]. Cho et al. [22] speculate that nominally pure $LiCoO_2$ is defective, and contains a small fraction of Co^{4+}, which could be compensated for by vacancies in the cobalt sublattices. According to these authors [22], the substitution of a tetravalent ion is possible in the interstitial Co^{4+} sites. Thus, we expect Si^{4+} to form a small amount of $LiSi_yCo_{1-y}O_{2+0.5y}$.

The values of the R-factor, as defined by Dahn and co-workers [25,26], were 0.52, 0.51, 0.49, 0.55 and 0.78 for coating levels of 0.0, 0.3, 1.0, 3.0 and 5.0 wt.%, respectively. According to Dahn and co-workers [25,26], the lower the R-factor, the better the hexagonal ordering and, hence, the electrochemical performance. It can be seen that the R-value decreases slightly up to the 1.0 wt.% coating level and then rises. As we will see below, the electrochemical behavior of the coated samples are in agreement with this trend in the values of the R-factor.

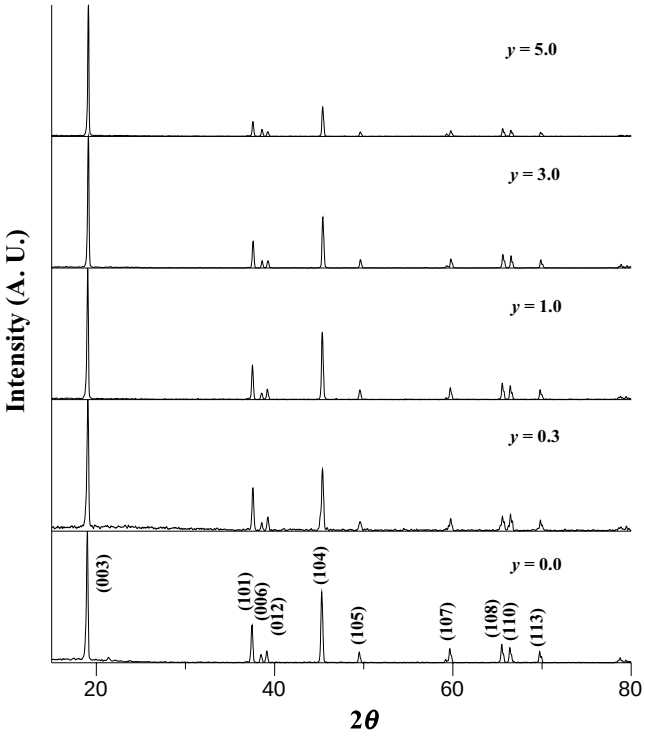

Fig. 2. X-ray diffraction patterns of the bare and coated Com-A $LiCoO_2$ powders.

3.2. Morphology

SEM images of the various coated Com-A $LiCoO_2$ powders are shown in Fig. 3. The texture of the surface of the cathode particles appears distinctly changed upon coating. The increasing brightness of the materials observed in these pictures as the coating level increased is associated with the accumulation of charge on the non-conducting coating material as the electron beam impinges on it. It can be seen that at low concentrations (0.3 and 1.0 wt.%) the coating is uniform. However, at higher coating levels small, loosely held agglomerates of the coating material were found glued to the surface, which suggests that at the 3.0 and 5.0 wt.% coating levels, the amount of fumed silica is more than what is required to form a uniform coating on the cathode powder, and that the excess silica agglomerates into small globules on the surface. Thus, it appears that a coating level of 1.0 wt.% or less would be sufficient to impart a uniform coating on the cathode powder. Fig. 4 shows the TEM image of a coated

Table 1
Lattice constants and R-factor values of the uncoated and silica-coated Com-A $LiCoO_2$

Composition	y	a (Å)	c (Å)	c/a	R-factor	Unit cell volume (Å)^3
$(100-y)$ wt.% Com-A	0.0	2.840 ± 0.009	13.982 ± 0.017	4.93 ± 0.03	0.51 ± 0.03	98.01 ± 0.04
+ (y) wt.% silica	0.3	2.835 ± 0.021	13.977 ± 0.017	4.93 ± 0.03	0.53 ± 0.05	97.28 ± 1.56
	1.0	2.831 ± 0.016	13.984 ± 0.012	4.94 ± 0.03	0.50 ± 0.02	97.03 ± 1.17
	3.0	2.836 ± 0.023	13.991 ± 0.067	4.93 ± 0.02	0.58 ± 0.03	97.44 ± 2.04
	5.0	2.836 ± 0.024	14.006 ± 0.080	4.94 ± 0.01	0.62 ± 0.14	97.59 ± 2.18

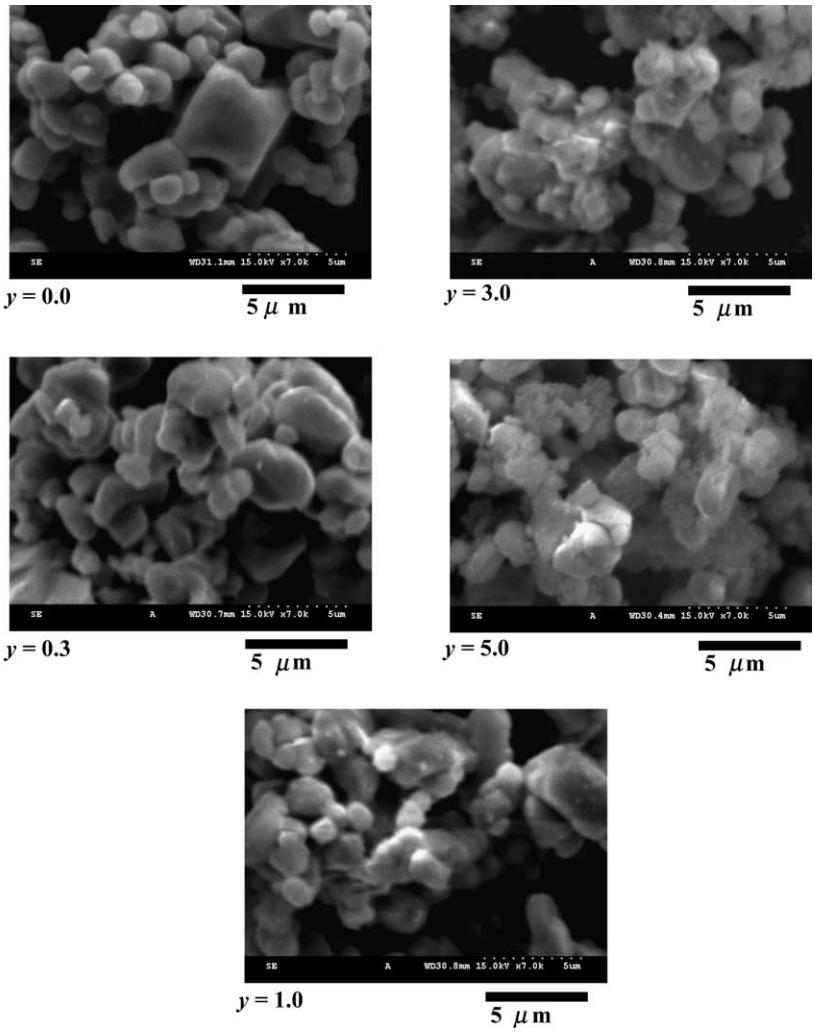

Fig. 3. SEM images of the various coated Com-A $LiCoO_2$ powders.

sample. The silica particles can be seen loosely bound to the surface. It is conceivable that during the calcination process, some of the silica species might diffuse into the bulk, resulting in the formation of solid solutions.

The BET surface areas of the bare and the 1.0 wt.%-coated powders were 0.62 and 4.85 $m^2\,g^{-1}$. The higher surface area of the coated material is reflective of the larger specific surface area of the fumed silica. The surface area of fumed silica used was 165 $m^2\,g^{-1}$. Therefore, an increase in the surface area by about 4 $m^2\,g^{-1}$ is commensurate with a 1.0 wt.% of fumed silica particles distributed over the surface of the cathode particles.

3.3. ESCA

The spatial distribution of the coated material in the samples is displayed in the depth profiles presented in Fig. 5. The concentration of cobalt increased to a depth of about 20 nm and then leveled off. There was an attendant decrease in the silicon concentration, which nearly leveled off beyond 20 nm. Thus, it is clear that the surface of the particles was encapsulated in a silica-rich layer, and that any cobalt that may have been present on the surface is the result of a slow diffusion of the cations from the interior during the calcination process. As inferred from our XRD results, it is also possible that the cobalt on the surface may be part of the $LiSi_yCo_{1-y}O_{2+0.5y}$ substitutional compound formed upon calcination. Curiously, the concentration of silicon remained non-zero even deep into the bulk of the cathode particle. Thus, it is clear that silicon diffuses into the bulk of the $LiCoO_2$ matrix. Based on the atomic concentrations of cobalt, oxygen and silicon in the matrix, typically at a depth of 50 nm, a tentative composition of $Li_xSi_{0.12}Co_{0.79}O_{2.00}$ can be assigned to the material present at these depths.

3.4. Galvanostatic cycling

In order to study the effectiveness of our coating process on the cyclability of the cathode material, the galvanostatic cycling behavior of the bare Com-A sample was compared with the behavior of a 1.0 wt.% fumed silica-coated Com-A sample. However, the coated sample was not subjected to

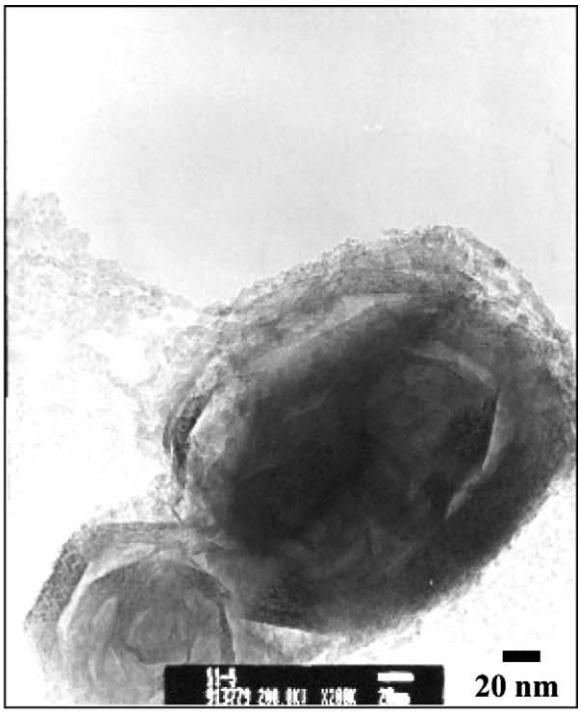

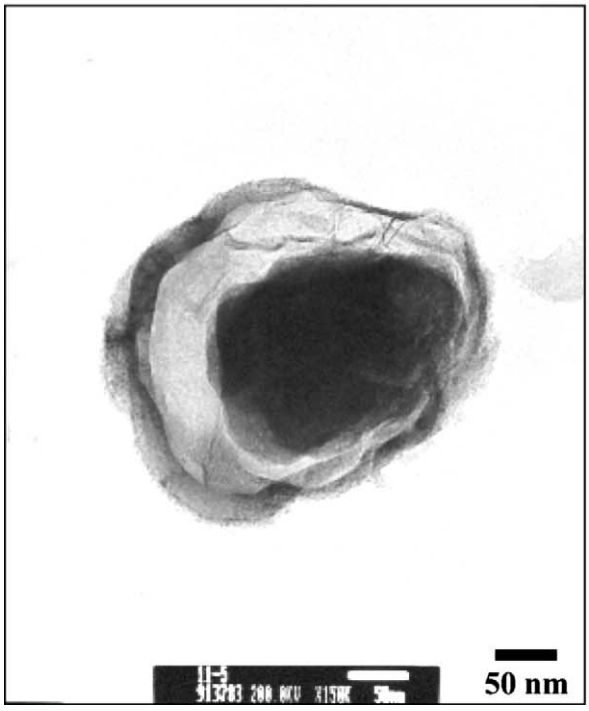

Fig. 4. TEM images of silica-coated Com-A $LiCoO_2$ particles.

calcination treatment. Fig. 6 compares the cycling behavior of the two materials. The cycling regime chosen was a 0.2*C* rate between 2.75 and 4.40 V. It can be seen that there was no improvement in the cyclability of the cathode material because of a loosely held layer of the coating material, which was both porous and fragile. Thus, we decided to calcine the coated sample so that the coating would strongly adhere to

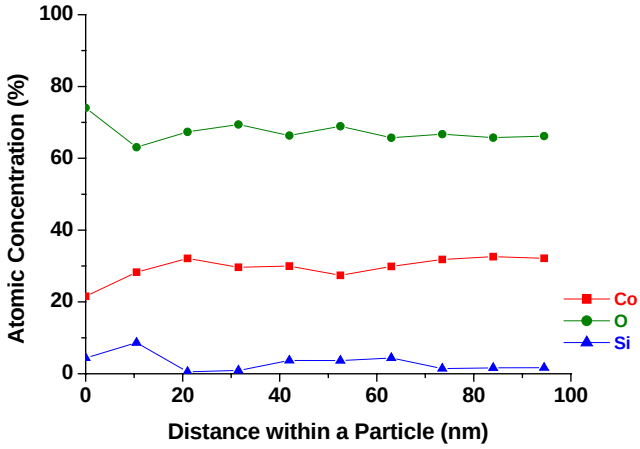

Fig. 5. Depth profiles of silicon, oxygen and cobalt in 1.0 wt.% silica-coated Com-A $LiCoO_2$.

the surface. The improved cycling behavior of the 1.0 wt.% fumed silica-coated calcined sample is depicted in Fig. 7. The first-cycle discharge capacity of the bare $LiCoO_2$ sample was 169 mAh/g, while those of the 0.3 and 1.0 wt.%-coated samples were 174 and 170 mAh/g, respectively. The slight increase in the capacity may be due to a better ordering of the core lattice, as exemplified by the *R*-factor data. However, when the coating levels were increased to 3.0 and 5.0 wt.%, the first discharge capacities dropped to 158 and 149 mAh/g, respectively, suggesting that as the coating level was increased, the capacity utilization of the cathode material fell. The drop in capacity at the high coating levels may have to do with the thickness of the coatings, which restricts the diffusion of lithium through the insulating layers. Additionally, the presence of excess coating material between the particles could lower the particle-to-particle electronic conductivity, and adversely affect the charging and discharging efficiencies.

Galvanostatic cycling data show that the coating improved the cyclability of the cathode material. For a cut-off value of 80% for the capacity retention, calculated with the first-cycle discharge capacity of the uncoated material as the reference, the number of cycles that the bare $LiCoO_2$ could sustain was 23. The cyclability rose to 33 and 70 cycles, respectively, for the materials 0.3 and 1.0 wt.% fumed silica. Obviously, a coating level of 0.3 wt.% was insufficient to impart a sufficiently compact coating. However, when the coating levels were increased further to 3.0 and 5.0 wt.%, the cyclability reduced. At the highest coating level employed (5.0 wt.%), the fall in the cyclability was precipitous, the material sustaining a mere seven cycles before reaching the 80% cut-off value. It is clear that the cyclability of the materials is commensurate with the trend in the variation of the *R*-factor as well as with their surface morphological features (Fig. 3). According to Courtright [27], thinner coatings produce smaller cracks that are a factor in controlling the ingress of molecular species. At the optimum coating level (1.0 wt.%), the cathode material registered nearly a three-fold increase in the cyclability.

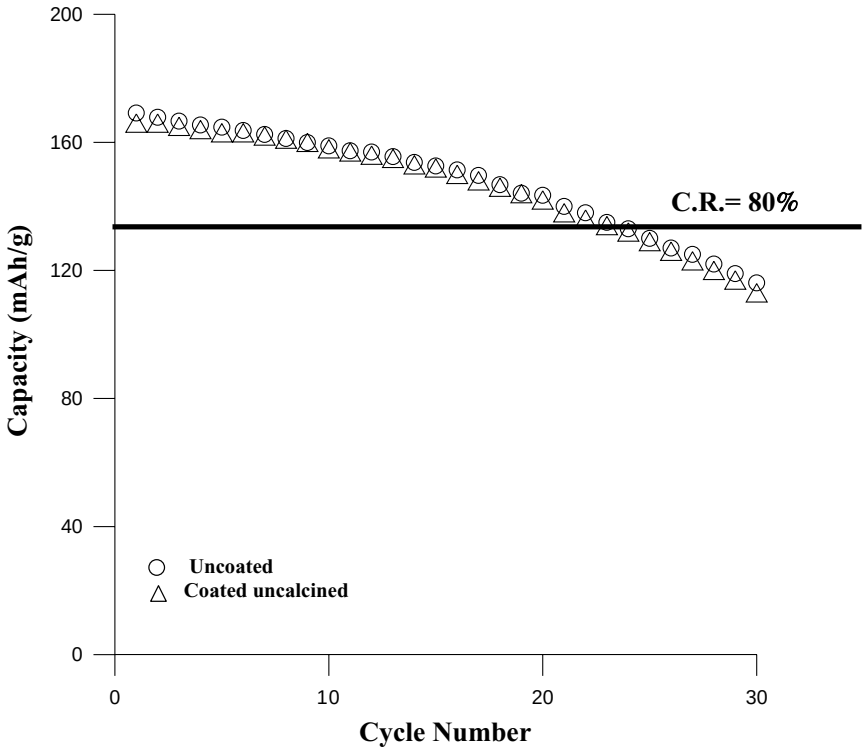

Fig. 6. Comparison of the cycling behavior of the bare and uncalcined 1.0 wt.% silica-coated Com-A $LiCoO_2$ samples. Charge–discharge: 0.2*C* rate between 2.75 and 4.40 V.

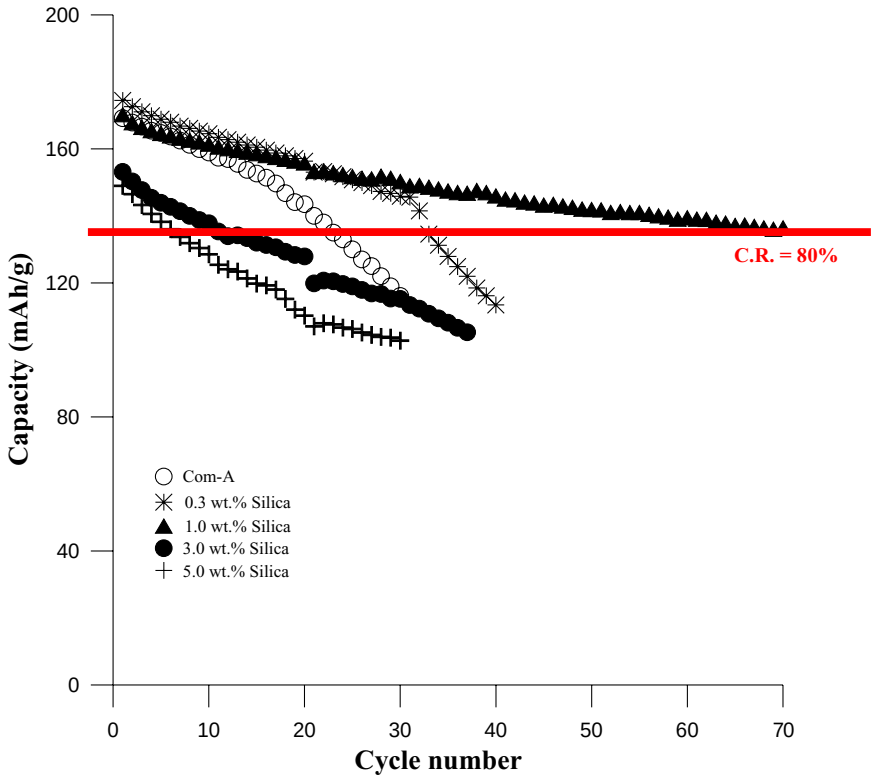

Fig. 7. Cycling behavior of bare and various silica-coated Com-A $LiCoO_2$ samples. Calcination: 450 °C for 10 h. Charge–discharge: 0.2*C* rate between 2.75 and 4.40 V.

3.5. Cyclic voltammetry

The deterioration in the cycling behavior of $LiCoO_2$ is believed to be due to a structural transition from a hexagonal phase to a monoclinic phase between 4.1 and 4.2 V versus Li^+/Li [7]. Accompanying this phase transition is a 1.2% expansion of the lattice in the *c*-direction, which is considered to be above the limit of ∼0.1% in elastic strain that oxides can tolerate [28]. Thus, slow scan cyclic voltammetry was performed in order to examine the effect of the coating on the phase transitions that accompany the charge–discharge processes. Fig. 8a shows the cyclic voltammogram of bare $LiCoO_2$, while Fig. 8b presents the one for 1.0 wt.% fumed silica-coated $LiCoO_2$. Although the first run of the cyclic voltammogram of the 1.0 wt.%-coated material showed hardly any change compared to the cyclic voltammogram of the bare sample, the peaks corresponding to the phase transitions seem suppressed beyond the second cycle. It appears that any defect in the coating gets repaired upon repeated cycling. The presence of cracks, pinholes, and other coating defects on coated surfaces is inevitable. It is conceivable that such defects may form and close with the

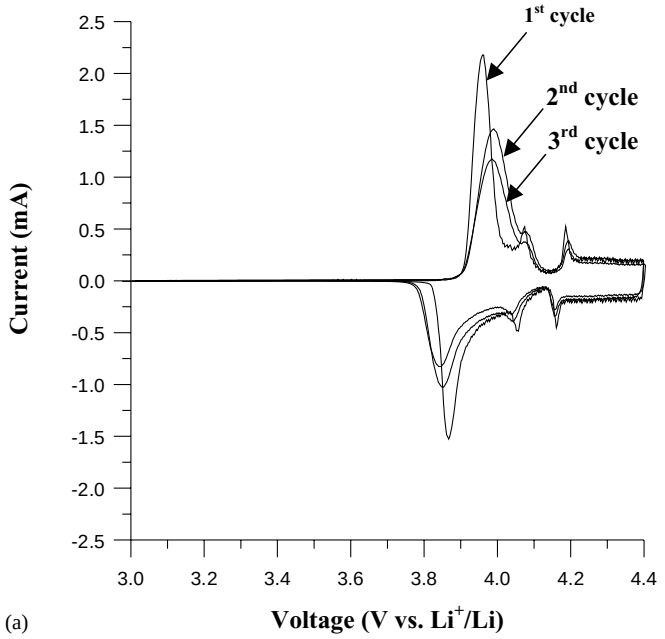

(a)

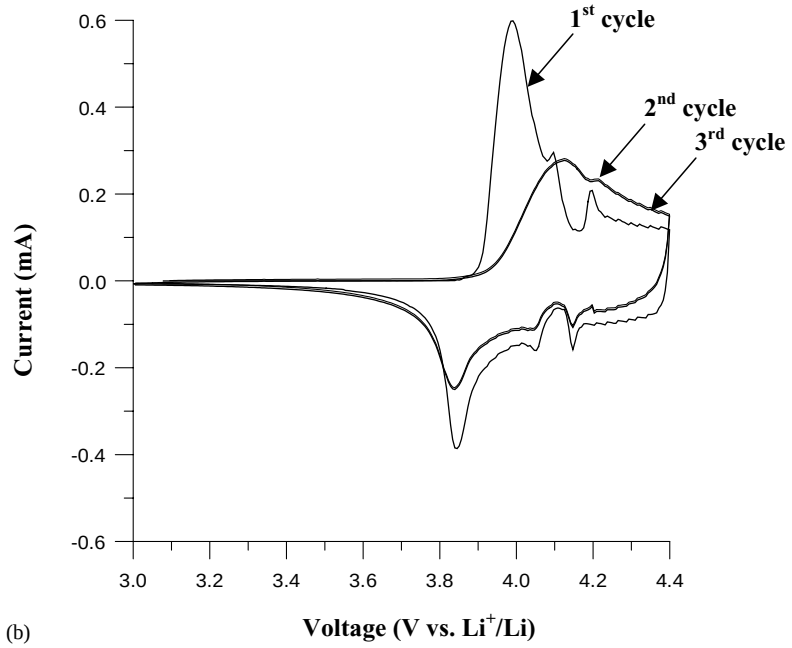

(b)

Fig. 8. Cyclic voltammogram of (a) bare Com-A $LiCoO_2$ and (b) 1.0 wt.% silica-coated Com-A $LiCoO_2$.

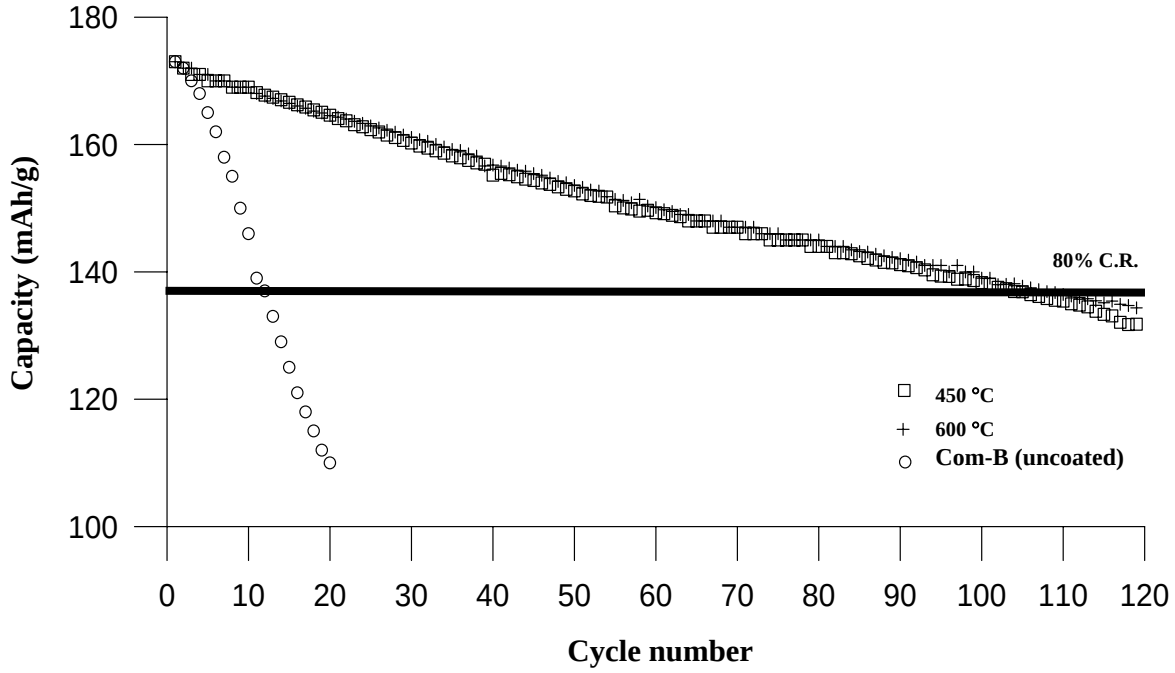

Fig. 9. Effect of calcination temperature on the cycling behavior of 1.0 wt.% silica-coated Com-B $LiCoO_2$ samples. Duration of calcination: 10 h. Charge–discharge: 0.1*C* rate between 2.75 and 4.40 V. The cycling behavior of an uncoated Com-B sample is given for comparison.

application of a load, or upon thermal cycling. In our case, changes in the surface texture that occurred as a result of the contraction and expansion of the lattice during the cycling process may have enabled the nanoparticulate coating material to become ingrained in the crevices and cracks on the cathode surface. The more compact kernel that resulted led to a suppression of the phase transitions, enhancing the cyclability of the coated material. In fact, it can be seen from Fig. 8b that from the second cycle onwards, the cyclic voltammogram of the coated material shows little evidence of such a transformation even at 4.4 V versus Li^+/Li.

3.6. Experiments with a second $LiCoO_2$ sample

Encouraged by the above results, a second sample of $LiCoO_2$ (Com-B) from the Coremax Taiwan Corporation was investigated as a core material for mechano-thermal coating with fumed silica. However, this time the charge–discharge cycling was done at a 0.1*C* rate, and only one coating level (1.0 wt.%) was considered. Additionally, the effect of calcination temperature on the cycling behavior was also studied. Fig. 9 compares the cycling behavior of the bare Com-B sample with those of the 1.0 wt.%-coated samples heat-treated at 450 and 600 °C. The Com-B $LiCoO_2$ sample gave a first-cycle capacity of 173 mAh/g, deteriorating to 138 mAh/g (the 80% capacity retention cut-off) in just 12 cycles. The first-cycle capacities of the coated samples were also 173 mAh/g. The silica-coated samples registered an 8–9-fold increase in cyclability. While the 450 °C-calcined sample sustained 101 cycles, the 600 °C-calcined sample sustained 104 cycles. The slightly larger number of cycles given by the 600 °C-calcined sample may be attributed to a more compact layer of the coating, formed by extended sintering. It is pertinent to note here that in addition to the economics and convenience of the coating procedure, the mechano-thermal process employs industrially manufactured pre-formed nanoparticles as coating materials, which makes its adaptability for commercialization attractive.

4. Conclusions

Pre-formed silica nanoparticles were coated on commercial $LiCoO_2$ cathode samples by a simple mechano-thermal coating process. Although the XRD patterns of the coated materials did not show any extraneous peaks corresponding to the coated particles, the slightly lower inter-layer distance, *c*, observed with the coated samples shows that a substitutional compound of the $LiSi_yCo_{1-y}O_{2+0.5y}$ type might have formed on the surface. SEM images showed the presence of small spherules of silica glued to the coated cathode particles at 3.0 and 5.0 wt.% coating levels, suggesting that such coating levels are above what is required for a uniform coating. TEM images of a 1.0 wt.%-coated particle suggested a partial diffusion of the silica species into the bulk of the particle. ESCA studies also showed that silicon was present in the bulk of the coated material, and that the concentration remained non-zero for a considerable depth, which suggests that the silica species diffused into the layer spacings in the cathode material. Cycling studies showed that at a coating level of 1.0 wt.%, the improvement in cyclability

was the greatest. The lowest *R*-factor value for this material supports the good structural stability of the 1.0 wt.%-coated sample, which confers the high cyclability. A 1.0 wt.% coating of silica particles enhanced the cyclability three-fold and nine-fold for samples Com-A and Com-B, respectively. Thus, the mechano-thermal process not only presents a simple and economical procedure for coating particulate substrates, but also has great potential for commercial adaptability, by virtue of the fact that it employs industrially manufactured pre-formed nanoparticles as coating materials.

Acknowledgements

Financial support for this work from the Industrial Technology Research Institute is gratefully acknowledged. TPK and SPN thank the National Science Council of the Republic of China for the award of post-doctoral fellowships.

References

[1] J.P. Parant, R. Olazcuga, M. Devalette, C. Fouassier, P. Hagenmuller, J. Solid State Chem. 3 (1971) 1.
[2] C. Fouassier, G. Matejka, J.M. Reau, P. Hagenmuller, J. Solid State Chem. 6 (1973) 532.
[3] K. Mizushima, P.C. Jones, P.J. Wiseman, J.B. Goodenough, Mater. Res. Bull. 15 (1980) 783.
[4] J.B. Goodenough, K. Mizushima, T. Takeda, Jpn. J. Appl. Phys. 19 (1980) 305.
[5] J.N. Reimers, J.R. Dahn, J. Electrochem. Soc. 139 (1992) 2091.
[6] T. Ohzuku, A. Ueda, J. Electrochem. Soc. 141 (1994) 2972.
[7] H.F. Wang, Y.I. Jang, B.Y. Huang, D.R. Sadoway, Y.M. Chiang, J. Electrochem. Soc. 146 (1999) 473.
[8] E. Plichita, S. Slane, M. Uchiyama, M. Salomon, D. Chua, W.B. Ebner, H.W. Lin, J. Electrochem. Soc. 136 (1989) 1865.
[9] G.G. Amatucci, J.M. Tarascon, L.C. Klein, Solid State Ionics 83 (1996) 167.
[10] G. Ceder, Y.M. Chiang, D.R. Sadoway, M.K. Aydinol, Y.I. Jang, B.Y. Huang, Nature 392 (1998) 694.
[11] Y.I. Jang, B.Y. Huang, H.F. Wang, D.R. Sadoway, G. Ceder, Y.M. Chiang, H. Liu, H. Tamura, J. Electrochem. Soc. 146 (1999) 862.
[12] W.S. Yoon, K.K. Lee, K.B. Kim, J. Electrochem. Soc. 147 (2000) 2023.
[13] P.S. Dobal, R.S. Katiyar, M.S. Tomar, A. Hidalgo, J. Mater. Res. 16 (2001) 1.
[14] C. Pouillerie, L. Croguennec, Ph. Biensan, P. Willmann, C. Delmas, J. Electrochem. Soc. 147 (2000) 2061.
[15] C. Pouillerie, L. Croguennec, C. Delmas, Solid State Ionics 132 (2000) 15.
[16] C. Julien, G.A. Nazri, A. Rougier, Solid State Ionics 135 (2000) 121.
[17] J. Cho, Y.J. Kim, B. Park, Chem. Mater. 12 (2000) 3788.
[18] J. Cho, Y.J. Kim, B. Park, J. Electrochem. Soc. 148 (2001) A1110.
[19] J. Cho, Y.J. Kim, T.-J. Kim, B. Park, Angew. Chem. Int. Ed. 40 (2001) 3367.
[20] M. Mladenov, R. Stoyanova, E. Zhecheva, S. Vassilev, Electrochem. Commun. 3 (2001) 410.
[21] Z. Wang, C. Wu, L. Liu, F. Wu, L. Chen, X. Huang, J. Electrochem. Soc. 149 (2002) A466.
[22] J. Cho, C.-S. Kim, S.-I. Yoo, Electrochem. Solid-State Lett. 3 (2000) 362.
[23] J. Cho, G.B. Kim, H.S. Lim, C.-S. Kim, S.-I. Yoo, Electrochem. Solid-State Lett. 2 (1999) 607.
[24] H.-J. Kweon, S.J. Kim, D.G. Park, J. Power Sources 88 (2000) 255.
[25] J.N. Reimers, E. Rossen, C.D. Jones, J.R. Dahn, Solid State Ionics 61 (1993) 335.
[26] J.R. Dahn, U. von Sacken, C.A. Michal, Solid State Ionics 44 (1990) 87.
[27] E.L. Courtright, Surf. Coat. Technol. 68–69 (1994) 116.
[28] L.H. van Vlack, Physical Ceramics for Engineers, Addison-Wesley, Reading, MA, 1964.